Public Health England

Evaluation of a Detector System for Measurement of Low Energy Photon Emitting Radionuclides in the Body

About Public Health England

Public Health England exists to protect and improve the nation's health and wellbeing, and reduce health inequalities. It does this through advocacy, partnerships, world-class science, knowledge and intelligence, and the delivery of specialist public health services. PHE is an operationally autonomous executive agency of the Department of Health.

Public Health England
133–155 Waterloo Road
Wellington House
London SE1 8UG
T: 020 7654 8000

www.gov.uk/phe
Twitter: @PHE_uk
Facebook: www.facebook.com/PublicHealthEngland

Any enquiries regarding this publication should be sent to

Press and Information
Centre for Radiation, Chemical and Environmental Hazards
Public Health England
Chilton, Didcot, Oxfordshire OX11 0RQ
E: ChiltonInformationOffice@phe.gov.uk

Published July 2014
PHE publications gateway number: 2014176

Evaluation of a Detector System for Measurement of Low Energy Photon Emitting Radionuclides in the Body

J E Scott

ABSTRACT

The objective of this work is to quantify the performance of an array of germanium detectors for measurement of low energy photon emitting radionuclides in the body. Calibrations have been completed for measurements of lead-210 and americium-241 in the skull and americium-241 and plutonium-239 in the lungs and liver. The calibrations are suitable for a wide range of subject sizes. The limits of detection for measurements of these radionuclides in the body have also been determined.

This development of the high resolution body monitoring system will provide Public Health England with improved, state-of-the-art capabilities for assessing intakes of radionuclides in the environment and in the workplace. This body monitoring system will also be a major resource for the response to any incident involving the release of alpha emitting low energy photon emitters (eg americium-241, plutonium-238 and plutonium-239) into the environment, which could arise from malevolent use incidents, or accidents involving transport of nuclear weapons or an installation with the potential to release such radionuclides.

This study was funded by the Centre for Research in Health Protection (CHPR) of the National Institute for Health Research (NIHR) under project no. 102077.

Centre for Radiation, Chemical and Environmental Hazards
Public Health England
Chilton, Didcot
Oxfordshire OX11 0RQ

Approval: May 2014
Publication: July 2014
£15.00
ISBN 978-0-85951-758-4

EXECUTIVE SUMMARY

The objective of this work is to quantify the performance of new germanium detectors for measurement of low energy photon emitting radionuclides in the body. New detector mounting plates have been developed, which allows rapid switching of the mounted detectors from those suitable for low energy photon emitters (such as plutonium-239 and americium-241) to a detector suitable for higher energy photon emitters (such as caesium-137 and cobalt-60), providing versatility within the same facility. Calibrations have been completed for measurements of americium-241 and lead-210 in the skull and americium-241 and plutonium-239 in the lung and liver, which are suitable for a wide range of subject sizes. The limits of detection for measurements of these radionuclides in people have also been determined and the committed effective doses corresponding to a selection of these limits of detection have been calculated for intakes by acute inhalation 1 day and 30 days before the measurement.

For measurements carried out between 1 day and 30 days following an intake, this body monitoring system is capable of detecting intakes corresponding to effective doses of under 10 mSv from measurements of:

a Lead-210 in skull (limit of detection, LOD = 14 Bq)

b Americium-241 in lungs (eg LOD = 5 Bq for chest wall thickness of 15.5 mm up to LOD = 11 Bq for chest wall thickness of 40.3 mm)

c Americium-241 in liver (LOD = 4 Bq for the lowest chest wall thickness of 15.5 mm)

For americium-241 in the skull, however, the LOD of 2–3 Bq measured 30 days after intake by inhalation corresponds to an effective dose of over 40 mSv: twice the annual dose limit for occupational exposure.

The sensitivity for intakes of pure plutonium-239 is comparatively poor compared to that for other radionuclides, with limits of detection for lungs and liver between 4 and 5 kBq at the lowest chest wall thickness, corresponding to effective doses of 2–3 Sv for measurements after 1 day for lungs and around 15 Sv for measurements after 30 days for liver, at best. However, as americium-241 is generally present with plutonium-239, monitoring for americium-241 can be used to infer intakes of plutonium, which correspond to much smaller doses than achievable with direct monitoring of plutonium-239.

This development of the high resolution body monitoring system provides Public Health England with state-of-the-art capabilities for assessing intakes of radionuclides in the environment and in the workplace. This body monitoring system will also be a major resource for the response to any incident involving the release of alpha emitting low energy photon emitters (eg americium-241, plutonium-238 and plutonium-239) into the environment, which could arise from malevolent use incidents, or accidents involving transport of nuclear weapons or an installation with the potential to release such radionuclides.

CONTENTS

1 INTRODUCTION

A new hyper-pure germanium (HPGe) detector system for *in-vivo* measurements has been installed in the low background laboratory at the Centre for Radiation, Chemical and Environmental Hazards of Public Health England, based at Chilton. The system comprises four p-type detectors of the Profile GEM-FX series (ORTEC model GEM-FX7025P4-RB). To minimise background radiation levels the system is housed in a low background steel room, the walls, door and roof of which are 150 mm thick and the base is 200 mm thick. Inside the room the walls are lined with 10 mm of aged lead and 2 mm of steel, which successively absorb scattered and characteristic radiation. Radon decay products are removed by a filtered recirculating air system, which provides about 25 changes of air per hour, of which up to 15% is fresh[1]. Measurements are carried out with the person seated in a specially designed chair fabricated from low background materials. Two detector mounts may each hold a pair of 83 mm diameter GEM-FX detectors for measurements of low energy photon emitters, or a single larger detector (ORTEC model GEM-90220-P-S) for whole body monitoring of high energy photon emitters. New detector mounting plates have been developed, which allow rapid switching of the mounted detectors from those suitable for low energy photon emitters [such as plutonium-239 (^{239}Pu) and americium-241 (^{241}Am)] to a detector suitable for higher energy photon emitters (such as caesium-137 and cobalt-60), providing versatility within the same facility. Each mount may be adjusted in the *x, y* and *z* directions, in the orthogonal angles θ and φ, and by rotation, ε, about the detector axis. This is required as low energy photon emitters such as ^{239}Pu and ^{241}Am tend to deposit in particular organs and so it is necessary to position these detectors over the organ of interest. A laser guide system has been developed to allow pairs of detectors to be accurately and reproducibly positioned over people. Axes are calibrated so that the mount positions may be recorded. The detectors are cooled using individual electrical coolers (ORTEC X-cooler II) housed on the roof of the steel room. The signals from the detectors are processed using Lynx digital signal analysers (Canberra) and analysed using Genie 2000 spectrometry software (Canberra). Routine quality assurance testing of the detectors checks that each detector's performance is acceptable.

The detector system has been calibrated for measurements of ^{239}Pu and ^{241}Am in lungs and liver and also for measurements of ^{241}Am and lead-210 (^{210}Pb) in skull. Lung and liver measurements are used to determine intakes of plutonium as insoluble plutonium compounds are retained in the lungs and, following absorption to blood, the liver is one of the main sites of deposition. Industrial sources of plutonium usually consist of a mixture of plutonium radionuclides and ^{241}Am from ingrowth from plutonium-241. Similarly, americium is also retained in the lungs and accumulates in the liver. Americium-241 emits higher energy (more penetrating) photons and is therefore much easier to detect in the body and is often used as a marker for intakes of mixtures of plutonium and americium. Americium-241 and plutonium are also deposited in bone and so measurements of the skull can be used to quantify intakes of ^{241}Am or mixtures of plutonium and americium. Such measurements can be particularly useful for historic intakes where much of the inhaled material may have cleared from the lungs. Direct measurements of ^{239}Pu in the skull are generally not carried out as the low energy photon emissions are strongly absorbed by bone. The skull is used for measurements of deposition in bone as it contains a high percentage of total bone in the body and has little overlying tissue.

Measurements of ^{210}Pb in the skull can be used to determine intakes of ^{210}Pb and in some cases can help to quantify long-term intakes of radon-222 which decays to ^{210}Pb.

The smallest amount of activity which can normally be detected is described by the limit of detection (LOD). The LOD for measurements of radionuclides in the body depends on many factors: the nature and thickness of overlying tissue, the energy and abundance of X-ray and gamma emissions, the size of thesensitive region of the detectors, the distance of the detectors from the body and the nature of insensitive absorbing layers between the body and the sensitive region of the detector. Limits of detection and effective doses which correspond to a measurement equal to the LOD for specified intake conditions have been determined.

2 EXPERIMENTAL DETAILS

2.1 Equipment

2.1.1 Detectors

The detectors are ORTEC Profile FX-Series GEM Coaxial P-type HPGe gamma-ray detectors in a reduced background PopTop capsule. The carbon fibre detector end-caps are 83 mm diameter and 0.76 mm thick, with an end-cap to detector distance of 5 mm. The crystal dimensions are approximately 70 x 25 mm (diameter x length). The manufacturer's reported operational range of these detectors is between 10 keV and 6 MeV. They are kept at liquid nitrogen temperature by individual electrical coolers mounted on top of the steel room. The steel room itself has been previously described in Knight et al[1] and Sumerling et al[2].

The four detectors are mounted in pairs on highly manoeuvrable, independent gantries allowing positioning at almost any co-ordinates and angle. Each type of adjustment has its own scale for ease of reproducibility.

The detector used for whole body measurements is described elsewhere[3].

2.1.2 Chair

A new chair for use with the detector system was sourced and installed. This chair was manufactured to our specification to ensure a person would be comfortable for the duration of the measurements and to hold the person in a precise location beneath the detectors. The materials used for the chair were selected to have low radionuclide contents to keep background levels in the counting environment as low as possible. The seat level and angle are fixed, but the back can be reclined (and the leg section raised) to the horizontal if necessary to provide a bed geometry. The usual angle of recline of the back for these measurements is 104 degrees.

2.2 Skull measurements

The phantoms used for the calibration of the GEM-FX detector system are two pairs of adult male human skulls with lower jaws on which known amounts of either ^{241}Am or ^{210}Pb have been uniformly deposited on the internal skull structures of one skull of each pair and on all the external skull structures of the other. The heads are similar in physical characteristics

including weight, circumference and width and are finished with tissue equivalent resin (New York University Medical Center). The circumference of the heads is about 590 mm.

The geometry used for the measurement was two pairs of detectors positioned either side of the head phantom, as illustrated in Figure 1.

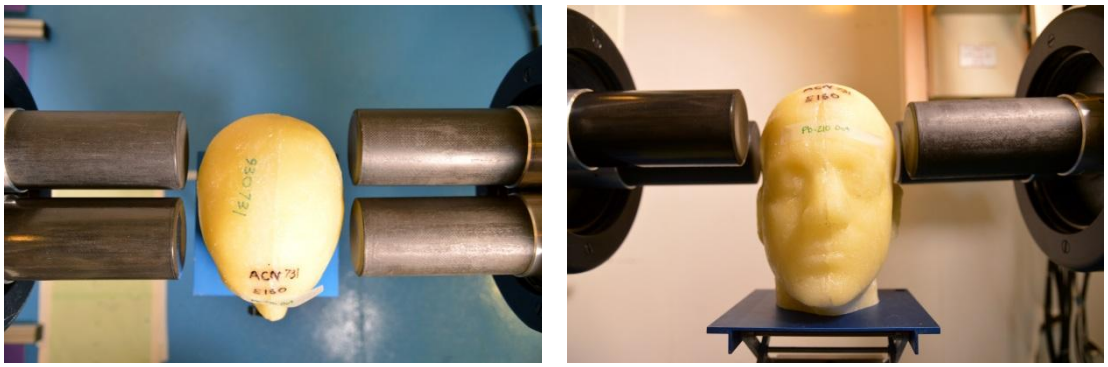

FIGURE 1 Head phantom showing position of GEM-FX detectors in relation to the skull

2.2.1 Background measurement

The background measurement was made using an inert head phantom composed of a plastic material. A single background measurement was carried out. The detector system and shielded room were set up with the blank head positioned as in Figure 1. Only peaks from naturally occurring radionuclides were observed in the acquired spectrum. The four individual detector spectra were summed and the background counts acquired in the regions of interest (ROI), as detailed in Appendix A.

2.2.2 Calibration measurements

The ^{210}Pb and ^{241}Am activities of the head phantoms are given in Table 1. A mean value from measurements of both internally and externally labelled skulls simulates realistic contamination of the bone mass.

TABLE 1 Activities of ^{241}Am and ^{210}Pb in head phantoms (Bq)

Nuclide	Exterior labelled skull	Interior labelled skull
^{241}Am	4,910	4,960
^{210}Pb	2,480	2,480

2.2.3 Measurement protocol

The support was positioned in the centre of the shielded room with respect to the detector gantries and the head phantom was placed on top (Figure 1) to raise the phantom to a height such that the detectors could be brought into the correct position.

Pairs of GEM-FX detectors were positioned so that the closest point of each detector end-cap was 1 cm from the surface of the head, just above the ear, at an inclination of 0 degrees. (See Figure 1 showing the position of the detectors relative to the head phantom.) For the ^{210}Pb phantom measurements only one pair of detectors was available, so separate measurements of the left and right side of the head had to be carried out in turn with the same detectors.

Count times were selected to give at least 5000 counts in the peaks at 60 keV (^{241}Am) and 47 keV (^{210}Pb).

2.3 Lung and liver measurements

In order to evaluate the GEM-FX detector system for the counting of ^{241}Am and ^{239}Pu in the lung and liver, a number of measurements were carried out using the Lawrence Livermore realistic thoracic phantom (LL phantom)[4].

The US Department of Energy's Committee for Low-Energy Photon Measurements recommended in 1974 the development of a phantom for use specifically in assessing lung contents of plutonium and certain other low energy photon emitting actinides. The work was undertaken by the Lawrence Livermore National Laboratory and a production version of the phantom was manufactured by Humanoid Systems Incorporated.

The LL phantom used is one of 16 second-generation phantoms produced for use by major laboratories involved in *in-vivo* measurement of transuranic nuclides. The basic composition of the phantom is commercial polyurethane, made to simulate the attenuation of uranium L X-rays (17 keV) in different tissues by the addition of appropriate concentrations of calcium carbonate. The phantom has interchangeable radio-labelled lungs and liver. Chest plate overlays, available in sets of four of increasing thickness, simulate one of three different chest wall compositions: 100% muscle; 50% adipose and 50% muscle; and 87% adipose and 13% muscle. In this work only the second type of overlay was used. The overlays are for placement over the phantom to allow simulation of chest wall attenuation of photon emissions for a variety of male statures.

FIGURE 2 Lawrence Livermore realistic thoracic phantom showing internal organs (lungs in black, liver to lower left), standard chest wall and one overlay

The chest plate and each overlay has three sets of concentric circles scribed over each lung and liver (Figure 2). These reference patterns are suggested for use as detector positioning guides. In addition, a 1 cm x 1 cm rectangular grid projected on the phantom surface provides reference co-ordinates for reproducing detector positions relative to the surface.

The overlays are designed to be used singly. However, for the purpose of achieving an estimated calibration for people of much larger stature it was decided to carry out an extra measurement using the two thickest overlays together. Due to the low energy of the ^{239}Pu emissions, attenuation with the thicker overlays had to be compensated for by lengthening count times considerably.

As the phantom was to be used in the 'seated' position and this phantom lacks the lower part of the torso, an empty Bottle Manikin Absorption (BOMAB) phantom[5,6] pelvis section was used to give a more realistic height. The LL phantom was stacked on top of the pelvis section, inside a support frame, on a purpose-built chair (Figure 3), the exact position and orientation of which were known and reproducible for each measurement.

FIGURE 3 Phantoms arranged on chair for lung measurement showing position of GEM-FX detectors in relation to the Lawrence Livermore phantom with no overlay

2.3.1 Background measurements

A single background measurement of the same duration as a usual subject measurement (2700 seconds) was carried out. The detector system and shielded room were set up as for a subject measurement with the LL phantom containing blank lungs and liver positioned on the chair as in Figure 3. Only peaks from naturally occurring radionuclides were observed in the acquired spectrum. The four individual detector spectra were summed and the background counts acquired in the regions of interest as detailed in Appendix A.

2.3.2 Investigation of crossfire

It was considered possible given the large area covered by the detectors in the lung and liver geometries that there could be a contribution to the signal from the non-target organ

(often termed crossfire). It was assumed the more weakly penetrating ^{239}Pu emissions would be much less likely to cause interference so only ^{241}Am organ phantoms were used to test for crossfire. One measurement was carried out with the detectors positioned for a lung measurement, but with blank lungs and the ^{241}Am liver in place, and one measurement with the detectors positioned for a liver measurement, but with a blank liver and ^{241}Am lungs in place. Each measurement was carried out with the chest plate alone. The detector efficiency for these measurements was calculated. The results are provided in Appendix E.

2.3.3 Calibration measurements

Calibration measurements were carried out for both the ^{241}Am and ^{239}Pu sets of lungs and livers, the activities of which are given in Table 2. For each set of radio-labelled phantoms six measurements of the LL phantom were carried out, with different overlays to represent people of different stature, as described in Table 3. Details of activity and physical characteristics are based on information provided by the manufacturer of the phantom at the time of purchase.

TABLE 2 Activities of ^{241}Am and ^{239}Pu in lung and liver phantoms (Bq)

Nuclide	Right lung	Left lung	Liver
^{241}Am	11,100	9,250	53,800
^{239}Pu	102,000	83,500	488,000

TABLE 3 Lawrence Livermore phantom configurations using overlays of tissue equivalent material representing 50% adipose/50% muscle (overlay set B124) to represent different statures

Configuration	Part/s in configuration	Chest wall thickness (mm)
Standard (no overlay)	LL chest (C-118P) BOMAB pelvis (empty)	Left side = 16.9 Right side = 14.5 Mean = 15.5
LL plus thinnest overlay	LL chest Overlay 124-1 BOMAB pelvis (empty)	Left side = 23.5 Right side = 21.0 Mean = 22.0
LL plus medium overlay	LL chest Overlay 124-2 BOMAB pelvis (empty)	Left side = 29.4 Right side = 27.3 Mean = 28.2
LL plus thicker overlay	LL chest Overlay 124-3 BOMAB pelvis (empty)	Left side = 34.2 Right side = 32.0 Mean = 32.9
LL plus thickest overlay	LL chest Overlay 124-4 BOMAB pelvis (empty)	Left side = 41.4 Right side = 39.6 Mean = 40.3
LL plus two thickest overlays	LL chest Overlay 124-4 Overlay 124-3 BOMAB pelvis (empty)	Left side = 58.7 Right side = 57.1 Mean = 57.7

2.3.4 Measurement protocol

The chair was positioned in the centre of the shielded room with respect to the detector gantries. The support frame containing the empty BOMAB phantom pelvis section was then placed on the chair in the centre at the back and the LL phantom was stacked on top leaning against the back of the chair (Figure 3). To hold the removable chest wall and successive overlays in position a strap was used around the body.

Pairs of GEM-FX detectors were positioned so that a laser pointed along the axis of the detectors created a light point at the centre of the guide circles on the LL phantom chest marking the centre of mass of each organ. The closest point of each detector end-cap was approximately 1 cm above the surface of the chest, as measured using a spacer. Figure 3 shows the positioning of the detectors relative to the LL phantom for the lung measurements and Figure 2 shows the targets for right and left lungs and liver. This procedure was repeated for each overlay configuration. Each of the configurations was measured for a minimum of 600 seconds; longer count times were used for weakly penetrating photons from ^{239}Pu and for thicker overlays.

3 RESULTS

All background data, calibration data and calculated detector efficiencies are given in the appendices. Individual detector results were summed for calculation of the limit of detection at each emission energy of interest.

3.1 Limits of detection

The limit of detection (LOD) in this report is the lowest activity which can be detected with 95% confidence during a 2700 second count time. The LOD for a particular emission energy was calculated as:

$$4.65\sqrt{B} / s\, e\, i$$

where B = background count in the ROI, s = count time in seconds, e = fractional counting efficiency and i = proportion of radioactive decays producing an emission (see Tables 4–8).

TABLE 4 Limits of detection for ^{241}Am and ^{210}Pb in skull (Bq) *(rounded to two significant figures)*

Nuclide	Emission energy (keV)	Skull and lower jaw only	Whole skeleton*
^{241}Am	60	2.2	17
^{210}Pb	47	14	100

* LOD for whole skeleton calculated using ratio of skull bone mass to total skeleton mass: see text

The detectable activities of both ^{241}Am at 60 keV and ^{210}Pb at 47 keV in the skull represent only a proportion of the radionuclide in the skeleton as a whole and thus the limits of detection presented must be interpreted as such. According to the International Commission on

Radiological Protection[7], the bones of the head (skull and lower jaw) constitute about 13% of the fresh skeleton by mass. The LOD for the skull must therefore be scaled up to 100% to represent an LOD for the whole skeleton.

TABLE 5 Limits of detection for ^{241}Am in lung (Bq) *(rounded to two significant figures)*

Emission energy (keV)	Chest wall thickness (mm)					
	15.5	22.0	28.2	32.9	40.3	57.7
60	4.7	6.4	7.1	8.5	11	21

TABLE 6 Limits of detection for ^{239}Pu in lung (Bq) *(rounded to two significant figures)*

Emission energy (keV)	Chest wall thickness (mm)					
	15.5	22.0	28.2	32.9	40.3	57.7
17	5,300	10,000	18,000	32,000	70,000*	400,000†
20	4,100	6,600	9,700	16,000	26,000	180,000†
52	6,700	9,800	11,000	11,000	16,000	33,000
129	26,000	33,000	36,000	34,000	55,000	84,000

* No peak identified at this energy by one detector: LOD calculated from results from three detectors

† No peak identified at this energy by two detectors: LOD calculated from results from two detectors

TABLE 7 Limits of detection for ^{241}Am in liver (Bq) *(rounded to two significant figures)*

Emission energy (keV)	Chest wall thickness (mm)					
	15.5	22.0	28.2	32.9	40.3	57.7
60	4.1	5.0	6.4	7.5	9.4	19

TABLE 8 Limits of detection for ^{239}Pu in liver (Bq) *(rounded to two significant figures)*

Emission energy (keV)	Chest wall thickness (mm)					
	15.5	22.0	28.2	32.9	40.3	57.7
17	4,600	9,000	16,000	30,000	66,000	360,000
20	4,700	7,500	11,000	16,000	31,000	120,000
52	5,700	6,300	8,900	10,000	13,000	26,000
129	20,000	21,000	30,000	32,000	41,000	76,000

4 DISCUSSION

A selection of the calculated limits of detection from this work have been used to determine the corresponding committed effective dose if this activity were to be measured in an adult 1 day and 30 days after intake by acute inhalation (Table 9). Dose calculations were made using the PHE computer code IMBA Professional Plus[8].

TABLE 9 Effective dose (mSv) corresponding to a measurement at the LOD at 1 day and 30 days after acute intake by inhalation* *(rounded to two significant figures)*

Nuclide	Energy (keV)	Skull†		Lung		Liver	
		1 day	30 days	1 day	30 days	1 day	30 days
^{210}Pb: Type M	47	9.2	5.4	–	–	–	–
^{241}Am: Type M	60	62	42	2.2	3.4	9.0	6.4
^{239}Pu: Type M	17	–	–	3,000	4,500	41,000	14,000
^{239}Pu: Type M	20	–	–	2,300	3,500	42,000	15,000
^{239}Pu: Type M	52	–	–	3,800	5,700	50,000	18,000
^{239}Pu: Type S	17	–	–	710	910	1,000,000	290,000
^{239}Pu: Type S	20	–	–	540	700	1,100,000	300,000
^{239}Pu: Type S	52	–	–	870	1,100	1,300,000	360,000

* Assumed activity median aerodynamic diameter of 5 µm; intake regime for Reference Worker light activity; and chest wall thickness of 15.5 mm

† Calculation from LOD for skeleton

Radionuclides such as ^{210}Pb, ^{241}Am and ^{239}Pu accumulate in bone and liver after acute intake, therefore the effective dose corresponding to a measurement at the LOD decreases with increasing time after intake. The effective doses corresponding to a measurement at the LOD for ^{210}Pb in skeleton at 1 day and 30 days after acute intake by inhalation are well within the 20 mSv annual dose limit for occupational exposure. For ^{241}Am, however, the dose corresponding to a skull measurement at the LOD is over three times the annual limit if measured 1 day after the intake and twice if measured 30 days after. Even 2 years after the intake a measurement equal to the LOD would indicate a dose exceeding the annual limit.

Conversely, the effective dose corresponding to a lung measurement at the LOD increases with increasing time after intake as the amount of radionuclide decreases due to lung clearance. The LOD for lung measurement of ^{241}Am at 60 keV is comparable with published detection levels[9] achieved by a number of facilities, ie 10 Bq, for a chest wall thickness of 40 mm. The increase in chest wall thickness from 15.5 mm to about 58 mm sees the LOD increase by about four times. Although for the lung these upper values still correspond to effective doses well within the annual dose limit for occupational exposure (20 mSv), for the liver this is true only up to a chest wall thickness of 40 mm.

For ^{239}Pu the attenuation due to a greater chest wall thickness was so great for measurements of activity in the lung that photon spectrum peaks were not discernible by at least one of the pair of detectors over the less active left lung. This resulted in lower calculated summed efficiencies and hence elevated limits of detection. However, as all the limits of detection of ^{239}Pu in both lung and liver correspond to levels well above the 20 mSv annual dose limit for occupational exposure (Table 9 shows some examples), this would not be considered a practical method of assessing dose due to intakes of this radionuclide. It is more usual that monitoring is carried out for ^{241}Am and the plutonium body content inferred from the ratio of the nuclides, which is often assumed to be 1 : 10 (Am : Pu) for occupational exposures, although higher ratios would be used in the case of a nuclear weapons accident. From Table 9 it can be seen that even in the most sensitive case (lung at 1 day after intake) this would still mean a dose from ^{239}Pu exceeding the 20 mSv annual limit. Even where this facility is not able to detect intakes corresponding to an effective dose of 20 mSv, measurements can still be valuable in determining if medical assessment is needed, as treatment is unlikely to be considered for effective doses less than 200 mSv[10].

5 CONCLUSIONS

Calibrations have been completed for measurements of ^{210}Pb and ^{241}Am in the skull, and ^{241}Am and ^{239}Pu in the lung and liver, suitable for a wide range of subject sizes. The limits of detection for measurements of these radionuclides in people have also been determined and the effective doses corresponding to a selection of those limits of detection have been calculated for specified intake conditions.

The GEM-FX detector system is capable of monitoring for ^{241}Am in the skull, lungs and liver down to just a few becquerels. For lung and liver, this corresponds to an effective dose of under 10 mSv if measured between 1 day and 30 days after acute intake by inhalation. This capability diminishes only slightly, to around 15 mSv, in heavily-built people with chest wall thicknesses of over 50 mm for measurement 30 days after intake. For the skull, however, 2–3 Bq measured up to 30 days after intake by inhalation corresponds to an effective dose of over 40 mSv: twice the annual dose limit for occupational exposure.

Conversely, detection of ^{210}Pb in the skull is a practical option as the LOD is only around 10 Bq, which corresponds to a total skeletal content of around 100 Bq and an effective dose of up to 10 mSv.

The capability of the system for direct lung or liver monitoring for ^{239}Pu is somewhat limited, as expected. With an intake by inhalation of around 430 Bq corresponding to a dose of about 20 mSv, even the lowest LOD for any of the plutonium energy emissions would be far in excess of occupational limits. However, in an emergency situation, perhaps associated with a nuclear weapons accident, where intakes could be high, it would be useful to monitor people to identify those who should be considered for treatment. It is more likely, however, that monitoring would be carried out for ^{241}Am and the plutonium body content inferred from the ratio of the nuclides; in this instance inference of effective doses in the order of tens of millisieverts may be achievable. All of the measurements described would be useful in identifying people who need medical assessment and possibly therapy to reduce the amount of radionuclide in the body.

This development of the high resolution body monitor provides Public Health England with improved, state-of-the-art capabilities for assessing exposures to radionuclides in the environment and in the workplace. This body monitoring system will also be a major resource for the response to any incident involving the release of alpha emitting low energy photon emitters (eg ^{241}Am, ^{238}Pu and ^{239}Pu) into the environment, which could arise from malevolent use incidents, or accidents involving transport of nuclear weapons or an installation with the potential to release such radionuclides.

6 ACKNOWLEDGEMENT

The author acknowledges the financial support of the Centre for Research in Health Protection (CHPR) of the National Institute for Health Research (NIHR) under project no. 102077 'Assessment of Intakes'. The views expressed in this publication are those of the author and not necessarily those of the NHS, the National Institute for Health Research or the Department of Health.

7 REFERENCES

1 Knight A, Fry FA, Whetmath PDJ and O'Riordan MC. Design and performance of major body monitoring facilities. Proceedings of 4th International Congress of the International Radiation Protection Association, Paris 1977; **2:** 537. http://www.irpa.net/irpa4/cdrom/VOL.2/P2_69.PDF.

2 Sumerling TJ, McClure DR and Massey DK. Measurement of total body radioactivity: the procedures used at the Board. Chilton, NRPB-R188, 1985.

3 Smith JRH, Marsh JW, Etherington G, Shutt AL and Youngman MJ. Evaluation of a high purity germanium detector body monitor. *Radiation Protection Dosimetry* 1994; **53**(1–4): 73–75.

4 Griffith RV, Dean PN, Anderson AL and Fisher JC. Fabrication of a tissue-equivalent torso phantom for intercalibration of *in vivo* transuranic nuclide counting facilities. In *Advances in Radiation Protection Monitoring.* Vienna, IAEA, STI/PUB/494, 1979, pp493–504.

5 ICRU. Phantoms and Computational Models in Therapy, Diagnosis and Protection. Bethesda MD, ICRU Report 48, 1992.

6 Health Physics Society. Specifications for the Bottle Manikin Absorption Phantom. American National Standard N13.35, 1999. http://hps.org/hpssc/N13_35_1999.html.

7 ICRP. Basic Anatomical and Physiological Data for Use in Radiological Protection: Reference Values. ICRP Publication 89. *Annals of the ICRP* 2002; **32**(3–4).

8 Birchall A, Puncher M, Marsh JW et al (2006). IMBA Professional Plus: a flexible approach to internal dosimetry. *Radiation Protection Dosimetry* 2007; **125**(1–4): 194–197.

9 Bérard Ph, Franck D, Dubiau C and Soulié R. Intercalibration of French lung monitoring systems for actinide measurements. *Radiation Protection Dosimetry* 2000; **89**(3–4): 235–238.

10 Rojas-Palma C, Liland A, Naess Jerstad A, Etherington G, Perez M and Rahola T. TMT Handbook. Triage, Monitoring and Treatment of People Exposed to Ionising Radiation Following a Malevolent Act, 2009. http://hera.helsebiblioteket.no/hera/handle/10143/96389.

APPENDIX A Background Measurements

A1 Chair background

Upon receipt of the new chair for the shielded room a measurement was carried out with the chair alone present in the room to ensure there were no anthropomorphic radioactive contaminants in the materials used. The spectrum acquired was similar to that of previous background results.

A2 Phantom backgrounds

The Lawrence Livermore phantom containing blank, non-radioactive, organs was set up in the shielded room as in Figure 3. Measurements were carried out using two pairs of p-type detectors of the Profile GEM-FX series (ORTEC model GEM-FX7025P4-RB) in the lung geometry and one pair of detectors in the liver geometry.

Background measurements for the skull were made using an inert head-shaped phantom composed of a plastic material. One pair of detectors was positioned on either side of the head as described previously (Section 2.2.1).

No peaks were observed in the resulting spectra except from naturally occurring radionuclides as shown in Table A1.

TABLE A1 Typical natural background peaks

Nuclide	Energy (keV)	Counts per second in ROI
^{212}Pb	238.6	0.006
^{214}Pb	295.2	0.009
^{214}Pb	351.9	0.011
Annihilation radiation*	511	0.012
^{214}Bi	609.3	0.010

* Annihilation radiation in this context refers to the gamma rays produced by an electron colliding with a positron

Individual detector spectra were summed for either lung, liver or skull measurements and a region of interest (ROI, Table A2) was set up for each of the emission energies to be studied for ^{241}Am, ^{239}Pu and ^{210}Pb. The number of counts in each ROI was established; this was then the background count for that region. To calculate the counts per second (cps) the peak net area (counts) was divided by the count time in seconds. For example, for a lung measurement, the summed counts for the four detectors for an ROI set up for determination of the 17 keV X-ray emissions of ^{239}Pu was 454 counts for a 2700 second measurement and the count rate in the ROI was determined by

$$cps_{(lung,\ 17\ keV)} = 454/2700 = 0.17$$

Similar data for all of the emissions is shown in Table A2.

TABLE A2 Background data

Nuclide	Peak energy (keV)	ROI (keV)	Counts in ROI			Counts per second in ROI		
			Lung	Liver	Skull	Lung	Liver	Skull
^{239}Pu	17	15.9–18.8	454	335	–	0.17	0.093	–
^{239}Pu	20	19.0–22.7	285	358	–	0.11	0.099	–
^{210}Pb	47	45.3–46.5	–	–	19	–	–	0.01
^{239}Pu	52	49.8–52.9	193	89	–	0.071	0.025	–
^{241}Am	60	57.7–61.2	236	113	92	0.087	0.031	0.046
^{239}Pu	129	127.9–131.5	204	90	–	0.076	0.025	–
Count time (seconds)			2,700	3,600	2,000			

APPENDIX B Skull Calibration Measurements

Results are presented for each GEM-FX detector used, named GEM1 to GEM4.

B1 Skull phantom calibration data

TABLE B1 ^{241}Am: skull phantom calibration data (cps) at 60 keV

		GEM1		GEM2		GEM3		GEM4	
Position of label	Count time (s)	Peak area	cps	Peak area	cps	Peak area	cps	Peak area	cps
External	2,000	26,120	13.06	26,583	13.29	17,839	8.92	21,730	10.87
Internal	2,000	22,291	11.15	19,047	9.52	15,543	7.77	19,395	9.70

TABLE B2 ^{210}Pb: skull phantom calibration data (cps) at 47 keV

		GEM1				GEM2			
		Left side of head		Right side of head		Left side of head		Right side of head	
Position of label	Count time (s)	Peak area	cps	Peak area	cps	Peak area	cps	Peak area	cps
External	25,000	19,648	0.79	9,293	0.37	7,751	0.31	26,620	1.06
Internal	25,000	14,080	0.56	9,984	0.40	8,116	0.32	16,095	0.64

B2 Detector efficiency for skull phantoms

The detector counting efficiency of each photon energy of interest was calculated for each skull phantom:

background subtracted cps / (total activity × fractional intensity of emission)

The fractional intensity is the proportion of decays which produce an emission of a photon. The skull phantom activities used for this work were given previously (Table 1).

TABLE B3 Fractional intensities for ^{241}Am and ^{210}Pb emission energies

Emission energy (keV)	Fractional intensity
47	0.043
60	0.359

B2.1 Detector efficiencies for skull measurements

TABLE B4 Detector efficiency: counts per second per ^{241}Am emission at 60 keV

Position of label	GEM1	GEM2	GEM3	GEM4	GEM-SUM*
External	0.0074	0.0075	0.0051	0.0062	0.0263
Internal	0.0063	0.0053	0.0044	0.0054	0.0215
Average					0.0239

* GEM-SUM = sum of all GEM-FX efficiencies

TABLE B5 Detector efficiency: counts per second per ^{210}Pb emission at 47 keV

	GEM1		GEM2		GEM-SUM*
Position of label	Left side of head	Right side of head	Left side of head	Right side of head	Left + right sides
External	0.0075	0.0035	0.0029	0.0101	0.0240
Internal	0.0053	0.0038	0.0031	0.0061	0.0183
Average					0.0212

* GEM-SUM = sum of all GEM-FX efficiencies

The difference between the efficiency of the detectors on the left and right sides of the head phantom can be attributed to their relative position. For the measurement on the right-hand side detector GEM1 was towards the back of the head and detector GEM2 at the front; these positions were reversed for the measurement of the left-hand side of the head, as the head was moved through 180 degrees rather than moving the detectors.

The reason why there should be a difference is less certain: the distance between the skull and the pair of detectors was defined as 1 cm at the closest point, which was just behind the ears, so the rear detector would have been slightly closer to the head than the front one on average due to the narrowing of the skull towards the face. This would have suggested a higher efficiency for detectors towards the back of the head; the reverse of the results above. It is possible that the distribution of the radioactive label is not uniform across the surfaces (external or internal) of the skulls.

APPENDIX C Lung Calibration Measurements

Where the number of counts in the peak was low, the peak search algorithm was sometimes unable to identify an appropriate ROI for a peak and in these cases the peak area was determined manually by positioning markers on either side of the peak. In a few cases it was not possible to identify a peak. Results are presented for each GEM-FX detector used, named GEM1 to GEM4.

C1 Lung phantom calibration data

TABLE C1 ^{241}Am: lung phantom calibration data (cps) at 60 keV

Chest wall thickness (mm)	Count time (s)	GEM1		GEM2		GEM3		GEM4	
		Peak area	cps	Peak area	cps	Peak area	cps	Peak area	cps
15.5	2,700	100,708	37.30	85,811	31.78	50,712	18.78	67,949	25.17
22.0	1,200	36,770	30.64	24,118	20.10	16,395	13.66	22,754	18.96
28.2	1,200	31,364	26.14	23,435	19.53	17,845	14.87	18,642	15.54
32.9	1,200	24,161	20.13	20,859	17.38	14,835	12.36	16,167	13.47
40.3	1,200	18,133	15.11	16,814	14.01	12,089	10.07	12,027	10.02
57.7	1,200	10,341	8.62	8,134	6.78	5,820	4.85	6,809	5.67

TABLE C2 ^{239}Pu: lung phantom calibration data (cps) at 17 keV

Chest wall thickness (mm)	Count time (s)	GEM1		GEM2		GEM3		GEM4	
		Peak area	cps	Peak area	cps	Peak area	cps	Peak area	cps
15.5	3,600	1,862	0.52	1,937*	0.54	298	0.08	484	0.13
22.0	4,500	1,324	0.29	1,058*	0.24	129*	0.03	423	0.09
28.2	5,400	694	0.13	902	0.17	195*	0.04	279	0.05
32.9	6,300	464	0.07	481*	0.08	223	0.04	152*	0.02
40.3	8,100	251*	0.03	498	0.06	–†		33*	0.00
57.7	28,800	223	0.01	265*	0.01	–†		–†	

* ROI set manually

† No peak identified

TABLE C3 ^{239}Pu: lung phantom calibration data (cps) at 20 keV

Chest wall thickness (mm)	Count time (s)	GEM1		GEM2		GEM3		GEM4	
		Peak area	cps	Peak area	cps	Peak area	cps	Peak area	cps
15.5	3,600	1,811	0.50	1,753*	0.49	420*	0.12	695	0.19
22.0	4,500	1,454*	0.32	1,312	0.29	231*	0.05	665	0.15
28.2	5,400	1,095	0.20	1,029	0.19	323*	0.06	569	0.11
32.9	6,300	700	0.11	725	0.12	337	0.05	356	0.06
40.3	8,100	556	0.07	600*	0.07	254	0.03	257*	0.03
57.7	28,800	594*	0.02	250*	0.01	–†		–†	

* ROI set manually

† No peak identified

TABLE C4 ^{239}Pu: lung phantom calibration data (cps) at 52 keV

Chest wall thickness (mm)	Count time (s)	GEM1		GEM2		GEM3		GEM4	
		Peak area	cps	Peak area	cps	Peak area	cps	Peak area	cps
15.5	3,600	772	0.21	636	0.18	458	0.13	524	0.15
22.0	4,500	696	0.15	524	0.12	332	0.07	475	0.11
28.2	5,400	643	0.12	606	0.11	367*	0.07	542	0.10
32.9	6,300	637*	0.10	791	0.13	479	0.08	592	0.09
40.3	8,100	594*	0.07	746	0.09	408	0.05	493	0.06
57.7	28,800	1,131	0.04	1,169	0.04	771	0.03	841	0.03

* ROI set manually

TABLE C5 ^{239}Pu: lung phantom calibration data (cps) at 129 keV

Chest wall thickness (mm)	Count time (s)	GEM1		GEM2		GEM3		GEM4	
		Peak area	cps	Peak area	cps	Peak area	cps	Peak area	cps
15.5	3,600	209	0.06	183	0.05	105	0.03	143	0.04
22.0	4,500	200*	0.04	146	0.03	126	0.03	155*	0.03
28.2	5,400	159	0.03	186	0.03	165	0.03	177	0.03
32.9	6,300	232	0.04	202	0.03	184	0.03	237	0.04
40.3	8,100	213	0.03	170	0.02	102*	0.01	191	0.02
57.7	28,800	385*	0.01	564	0.02	289*	0.01	327*	0.01

* ROI set manually

C2 Detector efficiency for lung phantom

The detector counting efficiency of each photon of interest was calculated for each phantom configuration of chest wall thickness:

background subtracted cps/ (total activity × fractional intensity of emission)

The fractional intensity is the proportion of decays which produce an emission of a photon. The lung phantom activities used for this work were given previously (Table 2).

TABLE C6 Fractional intensities for ^{241}Am and ^{239}Pu emission energies

Emission energy (keV)	Fractional intensity
17	0.016
20	0.0038
52	0.00027
60	0.359
129	0.000063

C2.1 Detector efficiencies for lung measurements

TABLE C7 Detector efficiency: counts per second per ^{241}Am emission at 60 keV

Chest wall thickness (mm)	GEM1	GEM2	GEM3	GEM4	GEM-SUM*
15.5	0.005	0.004	0.003	0.003	0.016
22.0	0.004	0.003	0.002	0.003	0.011
28.2	0.004	0.003	0.002	0.002	0.010
32.9	0.003	0.002	0.002	0.002	0.009
40.3	0.002	0.002	0.001	0.001	0.007
57.7	0.001	0.001	0.001	0.001	0.004

* GEM-SUM = sum of all GEM-FX efficiencies

TABLE C8 Detector efficiency: counts per second per ^{239}Pu emission at 17 keV

Chest wall thickness (mm)	GEM1	GEM2	GEM3	GEM4	GEM-SUM*
15.5	0.00018	0.00018	0.00003	0.00005	0.0004
22.0	0.00010	0.00008	0.00001	0.00003	0.0002
28.2	0.00004	0.00006	0.00001	0.00002	0.0001
32.9	0.00002	0.00003	0.00001	0.00001	0.00007
40.3	0.00001	0.00002	–†	0.000001	0.00003
57.7	0.000003	0.000003	–†	–†	0.000006

* GEM-SUM = sum of all GEM-FX efficiencies
† No peak identified

TABLE C9 Detector efficiency: counts per second per ^{239}Pu emission at 20 keV

Chest wall thickness (mm)	GEM1	GEM2	GEM3	GEM4	GEM-SUM*
15.5	0.00071	0.00069	0.00017	0.00027	0.0018
22.0	0.00046	0.00041	0.00007	0.00021	0.0012
28.2	0.00029	0.00027	0.00008	0.00015	0.0008
32.9	0.00016	0.00016	0.00008	0.00008	0.0005
40.3	0.00010	0.00011	0.00004	0.00005	0.0003
57.7	0.00003	0.00001	–†	–†	0.00004

* GEM-SUM = sum of all GEM-FX efficiencies

† No peak identified

TABLE C10 Detector efficiency: counts per second per ^{239}Pu emission at 52 keV

Chest wall thickness (mm)	GEM1	GEM2	GEM3	GEM4	GEM-SUM*
15.5	0.00429	0.00354	0.00255	0.00291	0.0133
22.0	0.00310	0.00233	0.00148	0.00211	0.0090
28.2	0.00238	0.00225	0.00136	0.00201	0.0080
32.9	0.00202	0.00251	0.00152	0.00188	0.0079
40.3	0.00147	0.00184	0.00101	0.00122	0.0055
57.7	0.00079	0.00081	0.00054	0.00058	0.0027

* GEM-SUM = sum of all GEM-FX efficiencies

TABLE C11 Detector efficiency: counts per second per ^{239}Pu emission at 129 keV

Chest wall thickness (mm)	GEM1	GEM2	GEM3	GEM4	GEM-SUM*
15.5	0.00496	0.00434	0.00249	0.00339	0.0152
22.0	0.00380	0.00277	0.00239	0.00294	0.0119
28.2	0.00252	0.00294	0.00261	0.00280	0.0109
32.9	0.00315	0.00274	0.00250	0.00321	0.0116
40.3	0.00225	0.00179	0.00108	0.00201	0.0071
57.7	0.00114	0.00167	0.00086	0.00097	0.0046

* GEM-SUM = sum of all GEM-FX efficiencies

APPENDIX D Liver Calibration Measurements

Results are presented for each GEM-FX detector used, named GEM1 and GEM2.

D1 Liver phantom calibration data

TABLE D1 ^{241}Am: liver phantom calibration data (cps) at 60 keV

Chest wall thickness (mm)	Count time (s)	GEM1		GEM2	
		Peak area	cps	Peak area	cps
15.5	600	64,907	108.18	57,597	96.00
22.0	600	54,296	90.49	47,779	79.63
28.2	600	42,814	71.36	37,187	61.98
32.9	600	35,122	58.54	31,930	53.22
40.3	600	28,158	46.93	24,549	40.92
57.7	600	14,746	24.58	12,525	45.27

TABLE D2 ^{239}Pu: liver phantom calibration data (cps) at 17 keV

Chest wall thickness (mm)	Count time (s)	GEM1		GEM2	
		Peak area	cps	Peak area	cps
15.5	3,600	4,567	1.27	5,799	1.61
22.0	4,500	2,794	0.62	3,792	0.84
28.2	5,400	2,072	0.38	2,443	0.45
32.9	6,300	1,273	0.20	1,561	0.25
40.3	8,100	764	0.09	891	0.11
57.7	28,800	494	0.02	407	0.01

TABLE D3 ^{239}Pu: liver phantom calibration data (cps) at 20 keV

Chest wall thickness (mm)	Count time (s)	GEM1		GEM2	
		Peak area	cps	Peak area	cps
15.5	3,600	4,966	1.38	5,415	1.50
22.0	4,500	3,810	0.85	4,561	1.01
28.2	5,400	3,160	0.59	3,378	0.63
32.9	6,300	2,564	0.41	2,714	0.43
40.3	8,100	1,415	0.17	2,008	0.25
57.7	28,800	1,213	0.04	1,756	0.06

TABLE D4 ^{239}Pu: liver phantom calibration data (cps) at 52 keV

Chest wall thickness (mm)	Count time (s)	GEM1		GEM2	
		Peak area	cps	Peak area	cps
15.5	3,600	2,246	0.62	2,081	0.58
22.0	4,500	2,337	0.52	2,525	0.56
28.2	5,400	2,137	0.40	2,063	0.38
32.9	6,300	2,214	0.35	2,231	0.35
40.3	8,100	2,205	0.27	2,110	0.26
57.7	28,800	3,874	0.13	3,958	0.14

TABLE D5 ^{239}Pu: liver phantom calibration data (cps) at 129 keV

Chest wall thickness (mm)	Count time (s)	GEM1		GEM2	
		Peak area	cps	Peak area	cps
15.5	3,600	618	0.17	616	0.17
22.0	4,500	696	0.15	714	0.16
28.2	5,400	657	0.12	632	0.12
32.9	6,300	622	0.10	716	0.11
40.3	8,100	708	0.09	655	0.08
57.7	28,800	1,413	0.05	1,191	0.04

D2 Detector efficiency for liver phantom

The detector counting efficiency for each photon emission of interest was calculated for each phantom configuration of chest wall thickness:

background subtracted cps / (total activity × fractional intensity of emission)

The fractional intensity is the proportion of decays which produce an emission of a photon. The liver phantom activities used for this work were given previously (Table 2).

D2.1 Detector efficiencies for liver measurements

TABLE D6 Detector efficiency: counts per second per ^{241}Am emission at 60 keV

Chest wall thickness (mm)	GEM1	GEM2	GEM-SUM*
15.5	0.006	0.005	0.011
22.0	0.005	0.004	0.009
28.2	0.004	0.003	0.007
32.9	0.003	0.003	0.006
40.3	0.002	0.002	0.005
57.7	0.001	0.001	0.002

* GEM-SUM = sum of all GEM-FX efficiencies

TABLE D7 Detector efficiency: counts per second per ^{239}Pu emission at 17 keV

Chest wall thickness (mm)	GEM1	GEM2	GEM-SUM*
15.5	0.00016	0.00021	0.00037
22.0	0.00008	0.00011	0.00019
28.2	0.00005	0.00006	0.00011
32.9	0.00003	0.00003	0.00006
40.3	0.00001	0.00001	0.00003
57.7	0.000002	0.000002	0.000005

* GEM-SUM = sum of all GEM-FX efficiencies

TABLE D8 Detector efficiency: counts per second per ^{239}Pu emission at 20 keV

Chest wall thickness (mm)	GEM1	GEM2	GEM-SUM*
15.5	0.00074	0.00081	0.00157
22.0	0.00046	0.00055	0.001
28.2	0.00032	0.00034	0.00067
32.9	0.00022	0.00023	0.00047
40.3	0.00009	0.00013	0.00024
57.7	0.00002	0.00003	0.00006

* GEM-SUM = sum of all GEM-FX efficiencies

TABLE D9 Detector efficiency: counts per second per ^{239}Pu emission at 52 keV

Chest wall thickness (mm)	GEM1	GEM2	GEM-SUM*
15.5	0.00475	0.00440	0.00921
22.0	0.00395	0.00427	0.00824
28.2	0.00301	0.00291	0.00585
32.9	0.00267	0.00270	0.00522
40.3	0.00207	0.00198	0.00387
57.7	0.00102	0.00105	0.00198

* GEM-SUM = sum of all GEM-FX efficiencies

TABLE D10 Detector efficiency: counts per second per ^{239}Pu emission at 129 keV

Chest wall thickness (mm)	GEM1	GEM2	GEM-SUM*
15.5	0.00558	0.00556	0.01100
22.0	0.00503	0.00516	0.01044
28.2	0.00395	0.00380	0.00760
32.9	0.00321	0.00369	0.00693
40.3	0.00284	0.00263	0.00548
57.7	0.00159	0.00134	0.00294

* GEM-SUM = sum of all GEM-FX efficiencies

APPENDIX E Crossfire Investigation

E1 Lung and liver phantom crossfire data

Results are presented for each GEM-FX detector used, named GEM1 to GEM4.

TABLE E1 ^{241}Am: liver phantom with measurement made in lung geometry (cps) at 60 keV

Chest wall thickness (mm)	Count time (s)	GEM1		GEM2		GEM3		GEM4		GEM-SUM*
		Peak area	cps	Peak area	cps	Peak area	cps	Peak area	cps	Efficiency
15.5	600	7,825	13.04	13,102	21.84	7,063	11.77	1,145	1.91	0.003

* GEM-SUM = sum of all GEM-FX efficiencies

TABLE E2 ^{241}Am: lung phantoms with measurement made in liver geometry (cps) at 60 keV

Chest wall thickness (mm)	Count time (s)	GEM1		GEM2		GEM-SUM*
		Peak area	cps	Peak area	cps	Efficiency
15.5	600	1,823	3.04	913	1.52	0.0006

* GEM-SUM = sum of all GEM-FX efficiencies

These efficiency results should be compared with those of the target organ alone with the same chest wall thickness, ie Tables C7 and D6. It can be seen that there is potential interference from crossfire radiation for measurements of ^{241}Am, but detectors placed over the lungs are a factor of five times more sensitive to activity in the lungs than to activity in the liver. In the reverse case, the detectors are around a factor of 20 times more sensitive to activity in the liver than the lungs for detectors placed over the liver.